Ab Initio Predictions of New Carbon Hypermagnesium Species: Mg_2C and Mg_3C

Alexander I. Boldyrev and Jack Simons*

Department of Chemistry, The University of Utah, Salt Lake City, Utah 84112

Received: May 30, 1996; In Final Form: September 20, 1996[⊗]

The ground and very low-lying excited states of new Mg_2C and Mg_3C molecules have been studied using high-level ab initio techniques. Four structures of Mg_2C, (C_{2v}, $^1A_1$), (C_{2v}, $^3B_1$), ($D_{\infty h}$, $^3\Sigma_g^-$), and ($D_{\infty h}$, $^5\Sigma_u^-$), were found to lie within 4 kcal/mol (at QCISD(T)/6-311+G(2df)) of one another. A C_{3v} ($^1A_1$) structure was found to be the only low-energy structure for Mg_3C. Both Mg_2C and Mg_3C were found to be thermodynamically stable with respect to all dissociation channels. Dissociation energies are found to be, for Mg_2C (C_{2v}, $^1A_1$) → MgC ($^3\Sigma^-$) + Mg (^1S), 24.6 kcal/mol and, for Mg_3C (C_{3v}, $^1A_1$) → Mg_2C (C_{2v}, $^1A_1$) + Mg (^1S), 41 kcal/mol at the QCISD(T)/6-311+G(2df)+ZPE level.

I. Introduction

Recently, the stable hypermagnesium oxides Mg_2O, Mg_2O^+, Mg_3O, and Mg_3O^+ have been studied theoretically[1,2] and experimentally.[3−7] While the usual valences of oxygen and magnesium are formally satisfied in MgO, it was somewhat surprising that the hyperstoichiometric molecules Mg_2O and Mg_3O were both found in theoretical and experimental studies to be quite stable. More recently, a hyperberrylium molecule Be_2O has also been studied theoretically[8,9] and experimentally[8] and was found to be thermodynamically very stable.

Two main factors have been found to be responsible for the stability of these hyperstoichiometric molecules. The first is the atomic charge on the oxygen (−1 instead of −2) in MgO and BeO, which makes it possible for oxygen to form one more bond such as those in Mg_2O and Be_2O, respectively. The second factor is the bonding interactions among the Mg centers in Mg_3O. With these thoughts in mind, we decided to see whether other hypermagnesium molecules with a different central atom could be stable. In particular, we decided to explore Mg_2C and Mg_3C because carbon, like oxygen, is multivalent and thus may be able to form various kinds of bonds with Mg in various charge states.

II. Computational Methods

The geometries and harmonic vibrational frequencies of Mg_2C and Mg_3C were first optimized by employing analytical gradients[10] with a polarized split-valence basis set (6-311+G* [11]) at the MP2 (full, including core orbitals and all double excitations) level. The geometries of Mg_2C were then reoptimized at the QCISD level with frozen C 1s and Mg 1s, 2s, and 2p orbitals, where numerical second derivatives were employed. The fundamental vibrational frequencies, normal coordinates, and zero-point energies (ZPE) were calculated by standard FG matrix methods. The resultant QCISD/6-311+G* geometries for Mg_2C and the MP2(full)/6-311+G* geometries for Mg_3C were then used to evaluate higher level *valence* electron correlation both by Møller−Plesset perturbation theory to full fourth order[12] and by the (U)QCISD(T) method[13] using 6-311+G-(2df) basis sets but with the C 1s and Mg 1s, 2s, and 2p orbitals now frozen. The unrestricted Hartree−Fock (UHF) wave functions for open-shell systems were projected to pure spectroscopic states (PUHF, PMP2, PMP3, and PMP4[14]). All calculations were carried out with the GAUSSIAN 94[15] suite of programs unless otherwise specified.

III. Results

A. MgC. This molecule was recently predicted computationally to have a $^3\Sigma^-$ ground electronic state with a valence electron configuration[16] denoted as $1\sigma^2 2\sigma^2 1\pi^2$ and a bond length and dissociation energy of 2.10 Å and 34.5 kcal/mol. Throughout this work, the C 1s and Mg 1s, 2s, and 2p core orbital occupancies could be represented as [ ] = $1\sigma^2 2\sigma^2 3\sigma^2 1\pi^4 4\sigma^2$ in which case the valence configuration given earlier would read [ ] = $5\sigma^2 6\sigma^2 2\pi^2$. However, we prefer to shorten the notation and to focus attention on the valence orbitals by (i) ignoring [ ] in writing the configuration and (ii) beginning the numbering of orbitals with the valence orbitals. Within this notational scheme, the lowest excited state was found to be the high-spin $^5\Sigma^-$ ($1\sigma^2 2\sigma^1 1\pi^2 3\sigma^1$) state, which lies just 10.5 kcal/mol above the $^3\Sigma^-$ state (all data at the QCISD(T)/6-311+G(2df) level detailed in section II.).

B. Mg_2C. For this molecule and for Mg_3C, we examined a wide variety of geometrical structures. In each case, we considered singlet, triplet, and quintet spin states and then focused only on candidates for the lowest energy states. This process generated twelve electronic state and geometrical structure combinations for Mg_2C at the MP2(full)/6-311+G* level: MgCMg ($D_{\infty h}$, $^1\Sigma_g^+$), MgCMg ($D_{\infty h}$, $^3\Sigma_g^-$), MgCMg ($D_{\infty h}$, $^5\Sigma_u^-$), Mg_2C (C_{2v}, $^1A_1$), Mg_2C (C_{2v}, $^3B_1$), Mg_2C (C_{2v}, $^3B_2$), Mg_2C (C_{2v}, $^3A_2$), Mg_2C (C_{2v}, $^5A_1$), Mg_2C (C_{2v}, $^5B_2$), CMgMg ($C_{\infty v}$, $^1\Sigma^+$), CMgMg ($C_{\infty v}$, $^3\Sigma^-$), and CMgMg ($C_{\infty v}$, $^5\Sigma^-$). The optimal geometries, vibrational frequencies, and relative energies for the lowest eight are presented in Table 1.

The MgCMg ($D_{\infty h}$, $^1\Sigma_g^+$) structure is found to be a saddle point (it has two imaginary frequencies) and is higher in energy (by 52.2 kcal/mol at QCISD/6-311+G*) than the (C_{2v}, $^1A_1$) minimum, which connects to this saddle point. In contrast, the MgCMg ($D_{\infty h}$, $^3\Sigma_g^-$), MgCMg ($D_{\infty h}$, $^5\Sigma_u^-$), CMgMg ($C_{\infty v}$, $^5\Sigma^-$), Mg_2C (C_{2v}, $^1A_1$), Mg_2C (C_v, $^3A_2$), Mg_2C (C_{2v}, $^3B_1$), Mg_2C (C_{2v}, $^3B_2$), and Mg_2C (C_{2v}, $^5A_1$) structures were found to be minima, and the Mg_2C (C_{2v}, $^1A_1$), MgCMg ($D_{\infty h}$, $^3\Sigma_g^+$), MgCMg ($D_{\infty h}$, $^5\Sigma_u^-$), CMgMg ($C_{\infty v}$, $^5\Sigma^-$), and Mg_2C (C_{2v}, $^3B_1$) structures were found to be substantially more stable than the others, as seen in Table 1.

[⊗] Abstract published in *Advance ACS Abstracts,* December 15, 1996.

S1089-5639(96)01586-1 CCC: $14.00

TABLE 1: Calculated Molecular Properties of Mg_2C

property	Mg_2C (C_{2v}, $^1A_1$) $1a_1^2 1b_2^2 1b_1^2 2a_1^2$	Mg_2C (C_{2v}, $^3B_1$) $1a_1^2 2a_1^2 1b_2^2 1b_1^1 3a_1^1$	MgCMg ($D_{\infty h}$, $^3\Sigma_g^-$) $1\sigma_g^2 1\sigma_u^2 2\sigma_g^2 1\pi_u^2$	MgCMg ($D_{\infty h}$, $^5\Sigma_u^-$) $1\sigma_g^2 1\sigma_u^2 2\sigma_g^1 1\pi_u^2 2\sigma_u^1$	Mg_2C (C_{2v}, $^3A_2$) $1a_1^2 1b_2^2 2a_1^2 1b_1^1 2b_2^1$	CMgMg ($C_{\infty v}$, $^5\Sigma^-$) $1\sigma^2 2\sigma^2 3\sigma^1 1\pi^2 4\sigma^1$	Mg_2C (C_{2v}, $^3B_2$) $1a_1^2 1b_2^2 2a_1^2 3a_1^1 2b_2^1$	Mg_2C (C_{2v}, $^5A_1$) $1a_1^2 1b_1^2 1b_2^1 2a_1^1 3a_1^1 2b_2^1$
				MP2(full)/6-311+G*//MP2(full)/6-311+G*				
R(Mg−Mg), Å	2.990	3.144	4.328	4.198	3.368	2.951	4.018	3.630
R(Mg−C), Å	2.047	2.127	2.164	2.099	2.156	2.072	2.113	2.043
$E_{mp2(full)}$, kcal/mol	−437.351 97	−437.326 14	−437.341 65	−437.368 20	−437.318 91	−437.336 67	−437.311 89	−437.292 53
$\langle S^2 \rangle$		2.997	2.585	6.039	2.856	6.031	2.034	6.055
ν_1, cm^{-1}	567 [$\nu_1(a_1)$]	415 [$\nu_1(a_1)$]	242 [$\nu_1(\sigma_g)$]	342 [$\nu_1(\sigma_g)$]	361 [$\nu_1(a_1)$]	593 [$\nu_1(\sigma)$]	462 [$\nu_1(a_1)$]	489 [$\nu_1(a_1)$]
ν_2, cm^{-1}	221 [$\nu_2(a_1)$]	127 [$\nu_2(a_1)$]	516 [$\nu_2(\sigma_u)$]	736 [$\nu_2(\sigma_u)$]	115 [$\nu_2(a_1)$]	221 [$\nu_2(\sigma)$]	100 [$\nu_2(a_1)$]	101 [$\nu_2(a_1)$]
ν_3, cm^{-1}	646 [$\nu_3(b_2)$]	512 [$\nu_3(b_2)$]	105 [$\nu_3(\pi_u)$]	148 [$\nu_3(\pi_u)$]	547 [$\nu_3(a_1)$]	95 [$\nu_3(\pi)$]	721 [$\nu_3(b_2)$]	682 [$\nu_3(b_2)$]
ZPE, kcal/mol	2.05	1.50	1.38	1.96	1.46	1.43	1.83	1.82
$\Delta E_{mp2(full)}$, kcal/mol	10.2	26.4	16.7	0.0	30.9	19.8	35.3	47.5
				QCISD/6-311+G*//QCISD/6-311+G*				
R(Mg−Mg), Å	2.999	3.168	4.308	4.220	3.456	2.967	3.605	3.555
R(Mg−C), Å	2.057	2.115	2.154	2.110	2.156	2.074	2.221	2.058
E_{qcisd}, kcal/mol	−437.107 82	−437.111 82	−437.112 44	−437.116 29	−437.09219	−437.09276	−437.06970	−437.04213
$\langle S^2 \rangle$		2.989	2.581	6.014	2.871	6.032	2.260	6.065
ν_1, cm^{-1}	548 [$\nu_1(a_1)$]	478 [$\nu_1(a_1)$]	274 [$\nu_1(\sigma_g)$]	326 [$\nu_1(\sigma_g)$]	401 [$\nu_1(a_1)$]	589 [$\nu_1(\sigma)$]		468 [$\nu_1(a_1)$]
ν_2, cm^{-1}	181 [$\nu_2(a_1)$]	126 [$\nu_2(a_1)$]	575 [$\nu_2(\sigma_u)$]	683 [$\nu_2(\sigma_u)$]	110 [$\nu_2(a_1)$]	209 [$\nu_2(\sigma)$]		102 [$\nu_2(a_1)$]
ν_3, cm^{-1}	598 [$\nu_3(b_2)$]	506 [$\nu_3(b_2)$]	74 [$\nu_3(\pi_u)$]	134 [$\nu_3(\pi_u)$]	596 [$\nu_3(b_2)$]	69 [$\nu_3(\pi)$]		650 [$\nu_3(b_2)$]
ZPE, kcal/mol	1.90	1.59	1.42	1.82	1.58	1.34		1.74
ΔE_{qcisd}, kcal/mol	5.3	2.8	2.4	0.0	15.1	14.8	29.2	46.5
				QCISD(T)/6-311+G(2df)//QCISD6-311+G*				
E_{mp2}, kcal/mol	−437.103 80	−437.081 02	−437.095 97	−437.119 78	−437.067 25	−437.083 16	−437.061 15	−437.047 49
E_{mp3}, kcal/mol	−437.105 15	−437.102 38	−437.118 15	−437.136 11	−437.091 76	−437.104 95	−437.082 27	−437.063 68
E_{mp4}, kcal/mol	−437.145 09	−437.118 85	−437.132 00	−437.144 50	−437.106 49	−437.112 58	−437.094 66	−437.072 66
E_{qcisd}, kcal/mol	−437.131 39	−437.133 46	−437.132 70	−437.138 92	−437.113 01	−437.110 94	−437.091 89	−437.067 13
$E_{qcisd(t)}$, kcal/mol	−437.152 92	−437.152 05	−437.149 86	−437.146 92	−437.130 41	−437.116 27	−437.102 15	−437.076 35
ΔE_{pmp4}, kcal/mol	0.0	16.5	8.2	0.4	24.2	20.4	31.6	45.5
$\Delta E_{qcisd(t)}$, kcal/mol	0.0	0.6	1.9	3.8	14.1	23.0	31.9	48.0

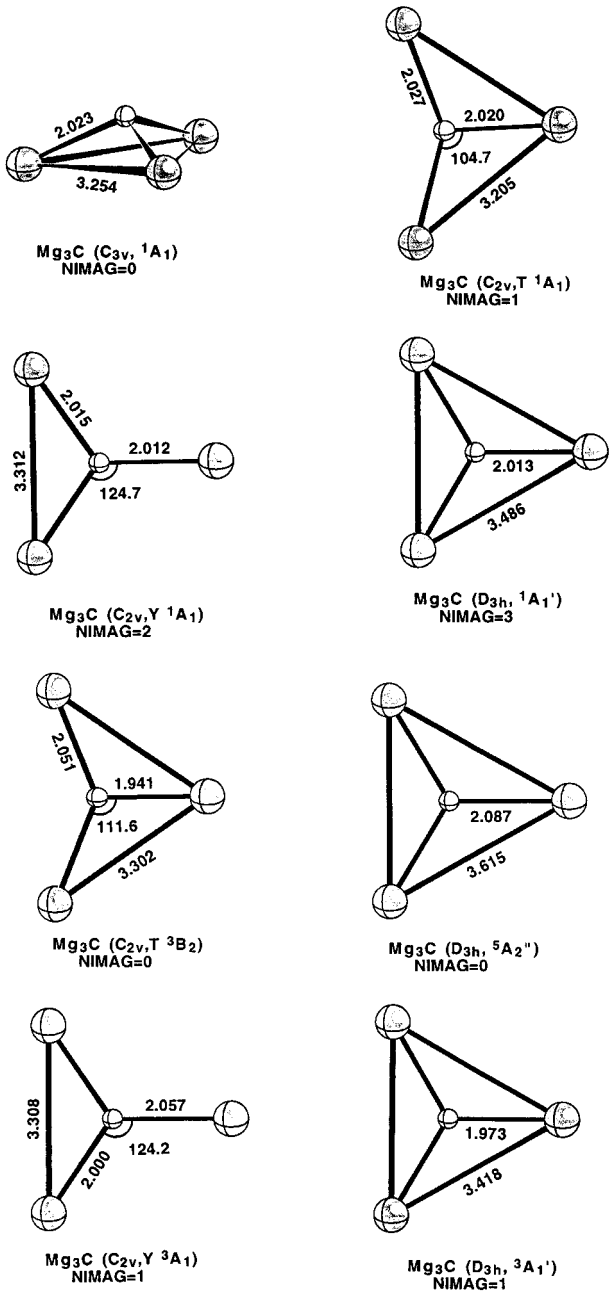

Figure 1. Optimized geometrical structures of Mg_3C (at MP2(full)/6-311+G*). Bond lengths are in angstroms and valence angles are in degrees.

At the MP2(full)/6-311+G* level of theory, the high-spin MgCMg ($D_{\infty h}$, $^5\Sigma_u^-$) structure is the most stable with Mg_2C (C_{2v}, $^1A_1$), MgCMg ($D_{\infty h}$, $^3\Sigma_g^-$), CMgMg ($C_{\infty v}$, $^5\Sigma^-$), and Mg_2C (C_{2v}, $^3B_1$) being 10.2, 16.7, 19.8, and 26.4 kcal/mol, respectively, higher in energy. However, at our highest level of theory (QCISD(T)/6-311+G(2df)), we found a different order of stability: the cyclic Mg_2C (C_{2v}, $^1A_1$) structure is the most stable and the four high-spin Mg_2C structures (C_{2v}, $^3B_1$), MgCMg ($D_{\infty h}$, $^3\Sigma_g^-$), MgCMg ($D_{\infty h}$, $^5\Sigma_u^-$), and CMgMg ($C_{\infty v}$, $^5\Sigma^-$) are 0.6, 1.9, 3.8, and 23 kcal/mol, respectively, higher in energy. Since the triplet states of Mg_2C have substantial spin contamination, we cannot predict with certainty which among them is the most stable, but it appears that the C_{2v} $^1A_1$ state is the lowest overall.

We calculated the dissociation energy D_e for the proported ground singlet Mg_2C (C_{2v}, $^1A_1$) state into MgC ($^3\Sigma^-$) + Mg (^1S) to be 24.6 kcal/mol at the QCISD(T)/6-311+G(2df)+ZPE level, which is close to the calculated dissociation energy D_e = 34.5 kcal/mol[16] of MgC ($^3\Sigma^-$).

TABLE 2: Calculated Molecular Properties of Mg_3C

property	Mg_3C (C_{3v}, $^1A_1$) $1a_1^2 1e^4 2a_1^2 3a_1^2$	Mg_3C (D_{3h}, $^1A_1'$) $1a_1'^2 1e''^4 1a_2''^2 2a_1'^2$	Mg_3C (C_{2v}, Y, $^1A_1$) $1a_1^2 2a_1^2 1b_2^2 1b_1^2 3a_1^2$	Mg_3C (C_{2v}, T, $^1A_1$) $1a_1^2 1b_2^2 2a_1^2 1b_1^2 3a_1^2$	Mg_3C (C_{2v}, T, $^3B_2$) $1a_1^2 1b_2^2 2a_1^2 1b_1^2 3a_1^1 2b_2^1$	Mg_3C (C_{2v}, Y, $^3A_1$) $1a_1^2 1b_2^2 2a_1^2 1b_1^2 3a_1^1 4a_1^1$	Mg_3C (D_{3h}, $^5A_2''$) $1a_1'^2 1e''^4 1a_2''^1 2e''^2 1a_1'^1$	Mg_3C (D_{3h}, $^3A_1'$) $1a_1'^2 1e''^4 1a_2''^2 2e''^2$
				MP2(full)/6-311+G*//MP2(full)/6-311+G*				
$E_{mp2(full)}$, kcal/mol	−637.211 68	−637.209 19	−637.209 25	−637.209 92	−637.181 68	−637.151 48	−637.169 91	−637.114 04
$\langle S^2 \rangle$					2.016	2.851	6.069	2.204
ν_1, cm^{-1}	505 [$\nu_1(a_1)$]	380 [$\nu_1(a_1')$]	781 [$\nu_1(a_1)$]	666 [$\nu_1(a_1)$]	815 [$\nu_1(a_1)$]	714 [($\nu_1(a_1)$]	347 [$\nu_1(a_1')$]	433 [($\nu_1(a_1')$]
ν_2, cm^{-1}	110 [$\nu_2(a_1)$]	151i [$\nu_2(a_2'')$]	380 [$\nu_2(a_1)$]	377 [$\nu_2(a_1)$]	370 [$\nu_2(a_1)$]	382 [$\nu_2(a_1)$]	168 [$\nu_2(a_2'')$]	1746i [$\nu_2(a_2'')$]
ν_3, cm^{-1}	688 [ν_3(e)]	752 [ν_3(e')]	54 [$\nu_3(a_1)$]	82 [$\nu_3(a_1)$]	107 [$\nu_3(a_1)$]	115 [$\nu_3(a_1)$]	671 [ν_3(e')]	955 [ν_3(e')]
ν_4, cm^{-1}	97 [ν_4(e)]	46i [ν_4(e')]	140i [$\nu_4(b_1)$]	51i [$\nu_4(b_1)$]	611 [$\nu_4(b_1)$]	148i [$\nu_4(b_1)$]	114 [ν_4(e')]	166 [ν_4(e')]
ν_5, cm^{-1}			717 [$\nu_5(b_2)$]	809 [$\nu_5(b_2)$]	698 [$\nu_5(b_2)$]	624 [$\nu_5(b_2)$]		
ν_6, cm^{-1}			61i [$\nu_6(b_2)$]	102 [$\nu_6(b_2)$]	172 [$\nu_6(b_2)$]	85 [$\nu_6(b_2)$]		
ZPE, kcal/mol	3.12	2.69	2.76	2.91		2.75	2.98	3.82
$\Delta E_{mp2(full)}$, kcal/mol	0.0	1.6	1.5	1.1	18.8	37.8	26.2	61.3
				QCISD(T)/6-311+G(2df)//MP2(full)/6-311+G*				
E_{pmp2}, kcal/mol	−636.841 50	−636.840 20	−636.840 23	−636.840 40	−636.813 17	−636.789 88	−636.799 96	−636.753 20
E_{pmp3}, kcal/mol	−636.818 35	−636.818 21	−636.818 12	−636.817 01	−636.802 97	−636.799 33	−636.812 51	−636.755 67
E_{pmp4}, kcal/mol	−636.873 59	−636.871 15	−636.871 24	−636.871 94	−636.842 18	−636.820 70	−636.827 75	−636.790 42
E_{qcisd}, kcal/mol	−636.828 24	−636.826 16	−636.826 14	−636.825 83	−636.813 43	−636.813 86	−636.816 23	−636.764 69
$E_{qcisd(t)}$, kcal/mol	−636.860 19	−636.858 42	−636.858 39	−636.858 29	−636.836 28	−636.832 05	−636.830 06	−636.796 17
$\langle S^2 \rangle$					2.016	2.851	6.069	2.204
ΔE_{pmp4}, kcal/mol	0.0	1.5	1.5	1.0	19.7	33.2	28.8	52.2
$\Delta E_{qcisd(t)}$, kcal/mol	0.0	1.1	1.1	1.2	15.0	17.7	18.9	40.2

TABLE 3: Calculated Effective Atomic Charges in MgC, CH_3MgH, Mg_2C, and Mg_3C

method	Q_C Mulliken[d]	Q(C−Mg) Mulliken	Q(Mg−Mg) Mulliken	Q_C dipole[e]	Q_C CHelpG[f]	Q_C MK[g]	Q_C NBO[h]	Q_{Mg} Mulliken[d]	Q_{Mg} dipole[e]	Q_{Mg} CHelpG[f]	Q_{Mg} MK[g]	Q_{Mg} NBO[h]
MgC ($^3\Sigma^-$)[a]												
MP2/6-311+G*	−0.311	0.155		−0.508	−0.496	−0.565	−0.856	+0.311	+0.508	+0.496	+0.565	+0.856
QCISD/6-311+G*	−0.290	0.177		−0.352	−0.373	−0.437	−0.734	+0.290	+0.352	+0.373	+0.437	+0.734
CH_3MgH (C_{3v}, $^1A_1$)[b]												
MP2/6-311+G*	−0.822	0.321		−0.922	−0.730	−0.881	−1.356	+0.673	+1.004	+0.911	+0.993	+1.463
QCISD/6-311+G*	−0.763	0.304		−0.896	−0.704	−0.852	−1.319	+0.644	+0.989	+0.896	+0.977	+1.445
HMgMgH ($D_{\infty h}$, $^1\Sigma_g^+$)[b]												
MP2/6-311+G*			0.466					+0.284	+0.381	+0.348	+0.381	+0.758
QCISD/6-311+G*			0.457					+0.268	+0.371	+0.338	+0.371	+0.737
CMg_2 (C_{2v}, $^1A_1$)[c]												
MP2/6-311+G*	−0.365	0.217	0.100	−0.733	−0.711	−0.850	−2.122	+0.183	+0.367	+0.356	+0.425	+1.061
QCISD/6-311+G*	−0.300	−0.006	0.271	−0.417	−0.526	−0.640	−1.885	+0.150	+0.209	+0.263	+0.320	+0.943
CMg_2 (C_{2v}, $^3B_1$)[c]												
MP2/6-311+G*	−0.161	−0.063	0.257	−0.419	−0.491	−0.601	−1.578	+0.081	+0.210	+0.246	+0.300	+0.789
QCISD/6-311+G*	−0.181	−0.054	0.228	−0.382	−0.453	−0.564	−1.538	+0.091	+0.191	+0.227	+0.282	+0.769
MgCMg ($^3\Sigma_g^-$)[c]												
MP2/6-311+G*	+0.147	−0.162		−0.365	−0.274	−0.365	−1.300	−0.074	+0.183	+0.137	+0.183	+0.650
QCISD/6-311+G*	−0.079	−0.001		−0.284	−0.220	−0.284	−1.346	+0.040	+0.142	+0.110	+0.142	+0.673
MgCMg ($^5\Sigma_u^-$)[c]												
MP2/6-311+G*	−0.455	0.293		−0.229	−0.209	−0.229	−1.621	+0.228	+0.115	+0.105	+0.115	+0.811
QCISD/6-311+G*	−0.409	0.249		−0.210	−0.187	−0.210	−1.546	+0.204	+0.105	+0.094	+0.105	+0.773
CMg_3 (C_{3v}, $^1A_1$)[b]												
MP2/6-311+G*	−0.195	−0.073	0.152	−0.885	−0.764	−0.927	−3.000	+0.065	+0.295	+0.255	+0.309	+1.000
QCISD/6-311+G*	−0.112	−0.184	0.184	−0.748	−0.745	−0.870	−2.877	+0.037	+0.249	+0.248	+0.290	+0.959

[a] At QCISD(T)/6-311+G(2df) geometry. [b] At MP2(full)/6-311+G* geometry. [c] At QCISD/6-311+G* geometry. [d] Mulliken population analysis. [e] Fitting charges to the potential, constrain them to reproduce the dipole moment. [f] Fitting charges to the potential at points selected according to the ChelpG scheme. [g] Fiting charges to the electrostatic potential at points selected according to the Merz−Singh−Kollman scheme. [h] Natural population analysis.

C. Mg_3C. For this stoichiometry, we also studied several structures and states as discussed earlier. This process caused us to focus on four singlets D_{3h} ($^1A_1'$: $1a_1'^2 1e'^4 1a_2''^2 2a_1'^2$), C_{3v} ($^1A_1$: $1a_1^2 1e^4 2a_1^2 3a_1^2$), C_{2v},T ($^1A_1$: $1a_1^2 1b_2^2 2a_1^2 1b_1^2 3a_1^2$), and C_{2v},Y ($^1A_1$: $1a_1^2 2a_1^2 1b_2^2 1b_1^2\ 3a_1^2$), three triplets C_{2v},T ($^3B_2$: $1a_1^2 1b_2^2 2a_1^2 1b_1^2 3a_1^1 1b_2^1$), C_{2v},Y ($^3A_1$: $1a_1^2 2a_1^2 1b_2^2 1b_1^2\ 3a_1^1 4a_1^1$), and D_{3h} ($^3A_1'$: $1a_1'^2 1e'^4 1a_2''^2 2e'^2$), and one quintet D_{3h} ($^5A_2''$: $1a_1'^2 1e'^4 1a_2''^1 2a_1'^1 2e'^2$).

We were not able to find any stable structure of C_{2v} symmetry with the carbon atom coordinated outside of a Mg_3 cluster. Upon geometry optimization such structures dissociated into Mg_2C + Mg. The final geometries (at the MP2(full)/6-311+G* level) of all of the stable Mg_3C structures that we were able to locate are shown in Figure 1 and their total and relative energies and harmonic frequencies are presented in Table 2.

According to our calculations, the singlet states lie lowest, with the pyramidal C_{3v} ($^1A_1$) structure the most stable. The D_{3h} ($^1A_1'$) planar structure was found to be a third-order saddle point and therefore cannot even be a transition state for the inversion of the C_{3v} ($^1A_1$) structure. Distortions of the D_{3h} ($^1A_1'$) species toward C_{2v} symmetry lead to two types of structures: C_{2v},T ($^1A_1$) and C_{2v},Y ($^1A_1$). The former is a true saddle point (with one imaginary frequency), and the second is a second-order saddle point.

However, at levels of theory above MP2 (see Table 2a), a D_{3h} ($^1A_1'$) structure was found to be the most stable singlet planar structure, and inversion of the C_{3v} ($^1A_1$) Mg_3C pyramid was found to occur through this D_{3h} ($^1A_1'$) structure. At our highest level of theory (QCISD(T)/6-311+G(2df)), the inversion barrier is only 1.11 kcal/mol (389 cm^{-1}). Considering the value of the inversion vibrational quantum 110 cm^{-1}, we expect that only three or four inversion vibrational levels are located below the barrier.

Among the low-energy triplet species identified, C_{2v},T ($^3B_2$), C_{2v},Y ($^3A_1$), and D_{3h} ($^3A_1'$), the first is a true local minimum with the others being saddle points. However, even the most stable triplet C_{2v},T ($^3B_2$) structure is less stable than the C_{3v} ($^1A_1$) global minimum structure by 15 kcal/mol. The lowest quintet, which is of D_{3h} ($^5A_2''$) structure, is a minimum but is higher in energy than the global minimum by 18.9 kcal/mol (all data at the QCISD(T)/6-311+G(2df) level).

We also calculated the dissociation energy D_e for the ground-state singlet Mg_3C (C_{3v}, $^1A_1$) state into ground-state singlet Mg_2C (C_{2v}, $^1A_1$) + Mg (^1S) to be 41 kcal/mol at the QCISD-(T)/6-311+G(2df)+ZPE level. Surprisingly, this dissociation energy of Mg_3C is larger than the Mg atom loss energies of Mg_2C (24.6 kcal/mol) and MgC (34.5 kcal/mol).

IV. Nature of the Bonding in MgC, Mg_2C, and Mg_3C

An ionic model for bonding in MgC transfers two electrons from Mg to C, giving Mg^{2+} (^1S), and C^{2-}(^3P) and predicts a $^3\Sigma^-$ ground state with atomic charges near ±2. Alternatively, a dative bonding picture describes MgC as involving a single two-electron dative bond with Mg serving as the electron pair donor and the empty 2p orbital of C the electron pair acceptor. This model also predicts a $^3\Sigma^-$ ground state. Both models view Mg as providing two valence electrons and *one* active valence orbital, and both leave the two unpaired electrons on the C center.

Allowing the Mg atom's electronic configuration to be "promoted" to $3s^1 3p^1$ and thus utilizing sp hybridization, MgC might be expected to have one σ bond, an sp σ unpaired electron on Mg, a nonbonding σ pair on C, and a pπ electron on C and hence a $^3\Pi$ state. However, this same promoted Mg $3s^1 3p^1$ configuration could combine with ^3P C to form one σ bond, a σ lone pair on C, and two pπ electrons (one from Mg and one from C) and thus a $^3\Sigma^-$ state. In this model, both the $^3\Pi$ and $^3\Sigma^-$ states have unpaired electron density on both Mg and C.

According to our calculations and those of others, the ground electronic state of MgC has two doubly occupied sigma ($1\sigma^2$

and $2\sigma^2$) orbitals and one partially occupied π orbital $(1\pi^2)^{16}$ composed almost completely of $2p_\pi$ AOs of the carbon atom. Only the 2σ MO has significant bonding character, so we view MgC as a singly bound species with its two unpaired nonbonding π electrons on C.

Additional information about the bonding can be obtained from atomic population analysis. Many different methods have been developed for the quantum chemical calculation of atomic charges. We explored five popular methods: Mulliken population analysis,[17] the Merz−Kollman method,[18,19] which produces partial charges fit to the electrostatic potential at points selected according to the Merz−Singh−Kollman scheme, the CHelpG method that produces charges fit to the electrostatic potential at points selected according to the CHelpG scheme,[19] the dipole method that produces charges to fit the potential constrained to reproduce the dipole moment,[20] and the natural bond analysis[21] method of Weinhold. We examined all of these methods to make certain that any conclusions we draw do not depend on using any *particular* definition of atomic charges.

A. MgC. Our results on MgC are presented in Table 3. As expected, the calculated effective atomic charges vary substantially from method to method, ranging from ±0.29 (Mulliken) to ±0.73 (NBO), all of which mean a substantial covalent character of the bonding in MgC. These charges can be compared with the atomic charges of C (varies from −0.76 (Mulliken) to −1.32 (NBO)) and Mg (varies from +0.64 (Mulliken) to +1.44 (NBO)) in CH_3MgH, where a single bond is clearly responsible for the Mg−C bonding. Also the overlap population $Q(\mathrm{Mg-C}) = 0.177$ in MgC is even lower than that, $Q(\mathrm{Mg-C}) = 0.304$, in CH_3MgH (at QCISD(T)/6-311+G*). The bond length of MgC ($^3\Sigma^-$) (R_e = 2.087 Å, at MP2(full)/6-311+G*) is very close to the Mg−C bond length in the CH_3−MgH molecule (R_e = 2.100 Å at the same level of theory), and the dissociation energy of MgC ($^3\Sigma^-$) into Mg (^{3}P) + C(^{3}P) (D_e = 94.6 kcal/mol) can be compared with the dissociation energy of the single Mg−C bond in CH_3MgH (into CH_3 + MgH; D_e = 64.9 kcal/mol, at QCISD(T)/6-311++G(2df,2pd)). From all of these data, one concludes that MgC has a *single* bond and atomic charges of less than ±1 (and certainly not close to ±2).

B. Mg_2C. As detailed in Table 3, in the most stable cyclic Mg_2C (C_{2v}, $^1A_1$) structure, the carbon has two Mg−C bonds and a lone pair, and the two magnesium atoms are bonded by a single Mg−Mg bond. The carbon center is thus much like an organic carbene.

As in conventional carbenes, one of the lone pair electrons on carbon can be promoted into the empty b_1 $p\pi$ orbital, producing a Mg_2C (C_{2v}, $^3B_1$) triplet state which is almost the same in energy. Both of the unpaired electrons in the Mg_2C (C_{2v}, $^3B_1$) state are located on the carbon atom according to our calculated spin densities.

C. Mg_3C. In the case of Mg_3C, the singlet (C_{3v}, $^1A_1$) structure has the lowest energy. In this molecule, the atomic charge on carbon is the most negative among the molecules studied and is −3.00 in the NBO scheme. Magnesium−magnesium bonding interactions are important contributors to the stability of this structure. Moreover, these interactions are responsible for an unusual flatness of the inversion potential energy surface in the area of the Mg_3C (D_{3h}, $^1A_1$) transition-state structure of this molecule. Overall, the ionic bonding between the valence unsaturated carbon atom and magnesium−magnesium bonding interactions are responsible for the stability of the hyperstoichiometric Mg_3C molecule in its C_{3v} ($^1A_1$) state.

Although we used sophisticated ab initio techniques in our computational predictions of new Mg_2C and Mg_3C molecules, experimental verification of our results are certainly desired.

Acknowledgment. This work was supported by NSF Grant No. CHE9116286.

References and Notes

(1) Boldyrev, A. I.; Shamovsky, I. L.; Schleyer, P. v. R. *J. Am. Chem. Soc*. **1992**, *114*, 6469.

(2) Boldyrev, A. I.; Simons, J.; Schleyer, P. v. R. *Chem. Phys. Lett*. **1995**, *233*, 266.

(3) Deng, H. T.; Okada, Y.; Foltin, M.; Castleman, A. W., Jr. *J. Phys. Chem.* **1994**, *98*, 9350.

(4) Ziemann, P. J.; Castleman, A. W., Jr. *J. Chem. Phys*. **1991**, *94*, 718.

(5) Ziemann, P. J.; Castleman, A. W., Jr. *Phys. Rev. B* **1991**, *44*, 6488.

(6) Ziemann, P. J.; Castleman, A. W., Jr. *Z. Phys. D* **1991**, *20*, 97.

(7) Ziemann, P. J.; Castleman, A. W., Jr. *Phys. Rev. B* **1992**, *46*, 482.

(8) Thompson, C. A.; Andrews, L. *J. Chem. Phys*. **1994**, *100*, 8689.

(9) Boldyrev, A. I.; Simons, J. *J. Phys. Chem*. **1995**, *99*, 15041.

(10) Schlegel, H. B. *J. Comput. Chem*. **1982**, *3*, 214.

(11) (a) Krishnan, R.; Binkley, J. S.; Seeger, R.; Pople, J. A. *J. Chem. Phys*. **1980**, *72*, 650. (b) McLean, A. D.; Chandler, G. S. *J. Chem. Phys*. **1980**, *72*, 5639. (c) Clark, T.; Chandrasekhar, J.; Spitznagel, G. W.; Schleyer, P. v. R. *J. Comput. Chem*. **1983**, *4*, 294. (d) Frisch, M. J.; Pople, J. A.; Binkley, J. S. *J. Chem. Phys*. **1984**, *80*, 3265.

(12) Pople, J. A.; Head-Gordon, M. Raghavachari, K. *J. Chem. Phys*. **1987**, *87*, 5968.

(13) Krishnan, R.; Pople, J. A. *Int. J. Quantum Chem*. **1978**, *14*, 91.

(14) Schlegel, H. B. *J. Chem. Phys*. **1984**, *84*, 4530.

(15) Frisch, M. J.; Trucks, G. W.; Schlegel, H. B.; Gill, P. M. W.; Johnson, B. G.; Robb, M. A.; Cheeseman, J. R.; Keith, T. A.; Peterson, G. A.; Montgomery, J. A.; Raghavachari, K.; Al-Laham, M. A.; Zakrzewski, V. G.; Ortiz, J. V.; Foresman, J. B.; Cioslowski, J.; Stefanov, B. B.; Nanayakkara, A.; Challacombe, M.; Peng, C. Y.; Ayala, P. Y.; Chem, W.; Wong, M. W.; Anders, J. L.; Replogle, E. S.; Gomperts, R.; Martin, R. L.; Fox, D. J.; Binkley, J. S.; DeFrees, D. J.; Baker, J.; Stewart, J. J. P.; Head-Gordon, M.; Gonzalez, C.; Pople J. A. *GAUSSIAN 94*, Revision A.1; Gaussian Inc.: Pittsburgh, PA, 1995.

(16) (a) Boldyrev, A. I.; Gonzales, N.; Simons, J. *J. Phys. Chem*. **1994**, *98*, 9931. (b) Bauschlicher, C. W., Jr.; Langhoff, S. R.; Partridge, H. *Chem. Phys. Lett.* **1993**, *216*, 341. (c) Da Silva, C. O.; Da Silva, E. C.; Nascimento, M. A. C. *Int. J. Quantum Chem., Quantum Chem. Symp*. **1995**, *29*, 639.

(17) Mulliken, R. S. *J. Chem. Phys*. **1955**, *23*, 1833.

(18) Besler, B. H.; Merz, K. M.; Kollman, P. *J. Comput. Chem*. **1990**, *11*, 431.

(19) Singh, U. C.; Kollman, P. A. *J. Comput. Chem*. **1984**, *5*, 129.

(20) Breneman, C. M.; Wiberg, K. B. *J. Comput. Chem*. **1990**, *11*, 361.

(21) Reed, A. E.; Curtiss, L. A.; Weinhold, F. *Chem. Rev.* **1988**, *88*, 899.